J Neuropathol Exp Neurol
Vol. 70, No. 5
May 2011
pp. 377–385

ORIGINAL ARTICLE

Transmission of Prion Strains in a Transgenic Mouse Model Overexpressing Human A53T Mutated α-Synuclein

Anne-Laure J. Mougenot, Anna Bencsik, PhD, Simon Nicot, Johann Vulin, Eric Morignat, Jérémy Verchère, Dominique Bétemps, PhD, Latefa Lakhdar, PhD, Stéphane Legastelois, PhD, and Thierry G. Baron, PhD, DVM

Abstract

There is a growing interest in the potential roles of misfolded protein interactions in neurodegeneration. To investigate this issue, we inoculated 3 prion strains intracerebrally into transgenic (TgM83) mice that overexpress human A53T α-synuclein. In comparison to nontransgenic controls, there was a striking decrease in the incubation periods of scrapie, classic and H-type bovine spongiform encephalopathies (C-BSE and H-BSE), with conservation of the histopathologic and biochemical features characterizing these 3 prion strains. TgM83 mice died of scrapie or C-BSE prion diseases before accumulating the insoluble and phosphorylated forms of α-synuclein specific to late stages of synucleinopathy. In contrast, the median incubation time for TgM83 mice inoculated with H-BSE was comparable to that observed when these mice were uninfected, thereby allowing the development of molecular alterations of α-synuclein. The last 4 mice of this cohort exhibited early accumulations of H-BSE prion protein along with α-synuclein pathology. The results indicate that a prion disease was triggered concomitantly with an overt synucleinopathy in some transgenic mice overexpressing human A53T α-synuclein after intracerebral inoculation with an H-BSE prion strain.

Key Words: α-Synuclein, Bovine spongiform encephalopathy, Prion, Scrapie.

INTRODUCTION

Accumulation of misfolded proteins is assumed to play a key role in the pathogenesis of many neurodegenerative disorders. The molecular pathway leading to synaptic dysfunction and neuronal death involves conformational changes in proteins that adopt β-sheet structures that are prone to oligomerization (1). The oligomers self-associate into toxic fibrils, which tend to become insoluble and protease-resistant, thereby generating aggregates that the proteolysis system fails to eliminate (2). This saturation of the cellular clearance system activates the apoptotic pathways that lead to major dysfunction and ultimately to cell death (3–6).

Among these protein-misfolding disorders, the transmissible spongiform encephalopathies (TSEs) are distinguishable from others by the fact that they can be transmitted between individuals and across species. The misfolded and aggregated form of prion protein (PrPd for disease-associated prion protein) is now accepted to be the major, if not the only, component that propagates these diseases by inducing the conversion of the normal host prion protein (PrPc) into its pathological conformer (7). Transmission studies in mice are widely used to characterize prion strains, which are defined by the mean incubation periods, the distribution and the intensity of the brain vacuolar lesions, the distribution and the type of PrPd, as well as the specific molecular pattern of PrPd (8–12).

In Parkinson disease (PD), the main protein involved in the pathological events causing neurodegeneration is α-synuclein. Point mutations and copy number variations in the gene encoding α-synuclein (*snca*) are associated with inherited forms of PD, thereby establishing a link between alterations and accumulation of this protein and the onset of disease (13–18). Moreover, fibrillized α-synuclein has been identified as the major constituent of intraneuronal aggregates, that is, ''Lewy bodies'' (19, 20). These inclusions rich in filamentous α-synuclein, combined with a substantial loss of neurons in the substantia nigra pars compacta, are hallmark lesions of PD.

However, as suggested by the overlap in the pathological and clinical features of patients with protein misfolding disorders (21, 22), the relationships between ''α-synuclein alterations and PD'' and between ''PrPd and prion diseases'' are not exclusive. Indeed, various misfolded neuronal proteins are present alongside α-synuclein in the brains of patients with PD (23). Conversely, pathological forms of α-synuclein can be detected concomitantly with PrPd in TSEs of humans (Creutzfeldt-Jakob disease [CJD]) or animals (scrapie) (22, 24–26). These findings raise questions about potential common mechanisms in the pathogenesis of prion and α-synuclein disorders.

The goal of this study was to provide a model of prion disease in mice prone to the development of a synucleinopathy. For this purpose, 3 different prion strains were transmitted by intracerebral (i.c.) inoculation into transgenic TgM83 mice that develop a motor phenotype during aging that is associated with the overexpression of human A53T mutated α-synuclein.

From the Agence Nationale de Sécurité Sanitaire de l'alimentation, de l'environnement et du travail – ANSES (A-LJM, AB, SN, JV, EM, JV, DB, LL, TGB), Lyon; and Indicia Biotechnology (A-LJM, SL), Oullins, France.

Send correspondence and reprint requests to: Thierry G. Baron, PhD, DVM, ANSES, 31 Avenue Tony Garnier, 69394 Lyon cedex 07, France; E-mail: thierry.baron@anses.fr

A.-L. J. M. was supported by a training grant (CIFRE 2006/1050) from the ANRT, Paris, France (Association Nationale pour la Recherche et la Technologie).

MATERIALS AND METHODS

Transgenic Mice and Prion Inoculation

For this study, we used a transgenic mouse model of synucleinopathy, that is, line TgM83, that overexpresses human A53T α-synuclein (B6; C3H-Tg[SNCA]83Vle/J, The Jackson Laboratory, Bar Harbor, ME) (27). We have observed that TgM83 mice spontaneously develop a dramatic motor phenotype between 10 and 22 months of age. At the end of life, TgM83 mice present characteristic clinical symptoms due to the α-synuclein pathology, including weight loss, reduced ambulation, severe motor impairment, prostration, and partial hind limb paralysis with overall stiffness of the hind legs and tail. The mice become unable to recover when placed on their back. We inoculated 6-week-old homozygous TgM83 mice (anesthetized by isoflurane inhalation) i.c. with 20 μL of 1% brain homogenates obtained from wild-type (wt) C57BL/6 mice with prion diseases (scrapie strain C506M3, classic bovine spongiform encephalopathy [C-BSE], or H-type BSE [H-BSE] [28, 29]). Nontransgenic C57BL/6 control mice (Charles River, L'Arbresle, France) were inoculated i.c. with the same prion strains. B6C3H mice (Charles River), which constituted the genetic background of the TgM83 mouse model, were also inoculated with the C-BSE strain at 1%. Age-matched control TgM83 mice that had not been inoculated with prions were killed either at 7 months of age (before the onset of clinical signs related to α-synuclein alterations), or at 14 months of age, after developing a severe motor phenotype due to synucleinopathy (27). The animals were cared for and housed in our approved experimental facilities (no. A 69 387 081), in accordance with the EC Directive 86/609/EEC for animal experiments and with the CREEA (Regional Committee for Ethical Experimentation on Animals—protocol no. 98). The mice were supplied with food and drink ad libitum and checked at least twice a week. Once they showed clinical signs, the animals were monitored daily and killed by administration of a lethal dose of sodium pentobarbital. The brains were removed, and one half was frozen and stored at −80°C for Western blot analyses and the other half was fixed in buffered formalin solution (10%, pH 7.4) for histopathologic analyses.

Extraction of PrP^{res}

The extraction methods used to identify and characterize the proteinase K (Roche, Meylan, France)–resistant prion protein (PrP^{res}) from mouse brains have been previously described (8, 29). Briefly, 20% brain homogenates were prepared in lysis buffer (50 mM Tris-HCl, pH 7.5, 150 mM NaCl, 5 mM EDTA). Proteinase K was added at a concentration of 10 μg per 100 mg of brain tissue, and samples were incubated at 37°C for 1 hour. *N*-lauroylsarcosyl (Sigma, Saint Quentin Fallavier, France) was added at a final concentration of 10%, and samples were then centrifuged at 465,000 × *g* for 2 hours over a 10% sucrose cushion. The pellet was resuspended in 50 μL of denaturing buffer TD4215 (4% SDS, 2% β-mercaptoethanol, 192 mM glycine, 25 mM Tris, 5% sucrose). In some experiments, deglycosylation was performed using PNGase F (P07043; Ozyme, Saint Quentin en Yvelines, France). Samples of PrP^{res} in TD4215 (1–2 μL) were mixed with denaturing buffer from the PNGase kit, G7 buffer, NP40, and PNGase according to the manufacturer's instructions. After incubation at 37°C for 1 hour, samples were ready for Western blot analysis after appropriate dilutions in TD4215 buffer.

Extraction of α-Synuclein

About 20% brain homogenates were prepared in high-salt buffer (50 mM Tris-HCl, pH 7.5, 750 mM NaCl, 5 mM EDTA, 1 mM DTT) containing 1% phosphatase (ref 78428; Fischer Scientific, Illkirch, France) and protease (P2714; Sigma) inhibitor cocktails. Samples were centrifuged at low speed (1,000 × *g* for 5 minutes at +4°C). About 200 μL of supernatants was incubated in *N*-lauroylsarcosyl at a final concentration of 10% before being ultracentrifuged at 465,000 × *g* (1 hour at +4°C) over a 10% sucrose cushion. The pellets (detergent-insoluble/SDS-soluble fraction) were resuspended in 50 μL of TD4215 buffer.

Western Blot Analysis

After heat denaturation for 5 minutes at 100°C in TD4215 buffer, proteins from the brain extracts were separated by electrophoresis using 15% SDS–polyacrylamide gels before being electroblotted onto poly vinylidene fluoride membranes (BioRad, Marnes La Coquette, France). Immunodetection of prion was performed with mouse monoclonal antibodies (mAb) Sha 31 (1:10 in PBST) (BioRad), 12B2 (340 ng/mL), or SAF 84 (500 ng/mL) (SPI-Bio, Montigny Le Bretonneux, France), respectively, directed against (144-WEDRYYRE-151), (88-WGQGG-92), and (163-RPVDQY-168) murine PrP sequences. α-Synuclein was probed with a rabbit mAb that only detects human α-synuclein phosphorylated on serine 129 (Pser129) (1:1000) (ref ab51253; Abcam, Cambridge, UK). The amount of proteins loaded on each lane was assessed by detection of GAPDH using a mouse mAb (1:10,000) (Millipore, Molsheim, France). Membranes were then incubated with horseradish peroxidase–conjugated goat anti-mouse (BioRad for Sha31 and ref 32430 [Fischer Scientific] for the other mouse mAb) or anti-rabbit (ref 32460; Fischer Scientific) secondary antibodies. The immunocomplexes were visualized with chemiluminescent reagents (ECL; GE Healthcare, Orsay, France), followed by exposure on Biomax MR Kodak films, or by analysis using the Versa Doc system and Quantity One software (both from BioRad). The apparent molecular weights were measured by comparing the positions of the bands with a biotinylated marker (B2787; Sigma) and the glycoform ratios of the PrP^{res} polypeptides were expressed as mean percentages (±SD) of the total signal for the 3 PrP^{res} glycoforms.

Lesion Profiles and Immunohistochemistry

After standard paraffin embedding, 5-μm brain sections were prepared. The slides were dewaxed then stained for either histopathologic or immunohistochemical examination. Slides stained with hematoxylin and eosin were evaluated for vacuolar lesions. Lesion profiles were determined according to Fraser and Dickinson's (30) lesion profile definition by quantification using a computer-assisted method (31). The PrPd deposition type and distribution were examined on immunostained brain slices using the SAF84 mAb (SPI-Bio), as previously described (9, 32, 33). Gliosis was analyzed on slices immunostained using a polyclonal antibody to glial fibrillary acidic protein

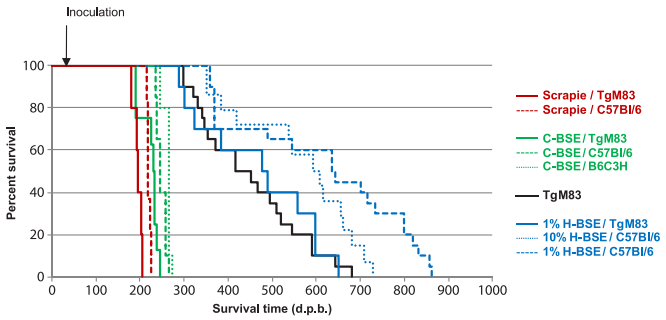

FIGURE 1. Kaplan-Meier survival curves for TgM83 mice and nontransgenic wild-type controls inoculated with scrapie C506M3, classic-type bovine spongiform encephalopathy (C-BSE), or H-type bovine spongiform encephalopathy (H-BSE) prion strains. TgM83 were inoculated i.c. at 6 weeks of age with 1% scrapie C506M3, 1% C-BSE, or 1% H-BSE. C57BL/6 mice were inoculated i.c. with 1% scrapie C506M3, 1% C-BSE, 1% H-BSE, or 10% H-BSE. B6C3H mice were inoculated with 1% C-BSE. Noninoculated TgM83 mice are also included. To allow comparisons of the groups inoculated with prion strains with the noninoculated TgM83 mice, the abscissa of this graph is expressed in days post birth (d.p.b.) representing the total survival times (from birth to death).

(Dako, Trappes, France), as described (9, 32, 33). Cells accumulating α-synuclein phosphorylated on serine 129 were detected using the Pser129 antibody. To enhance immunoreactivity for phosphorylated α-synuclein, sections were boiled in 0.1 mol/L of citrate buffer (pH 6.2) for 5 minutes using a microwave oven. Once refrigerated, the brain sections were immersed for 20 minutes in a 3-mol/L guanidine isothiocyanate solution to denature the proteins. After 3 washes in distilled water, endogenous peroxidase activity was blocked by a 5-minute immersion in 3% H_2O_2 solution. Primary antibody (Pser129) was applied at room temperature overnight (1:300) in a 0.1-mol/L saline phosphate buffer with 0.1× Triton. The secondary antibody (anti-rabbit; 1:200) was applied for 2 hours at room temperature. Antibody binding was detected using the avidin-biotin complex system (Vector Laboratories, Peterborough, UK) revealed by black deposition of 3, 3′ diaminobenzidine intensified with nickel chloride. The stained sections were observed under a light microscope BX51 (Olympus, Rungis, France) coupled to an image analysis workstation (MorphoExpert software; Explora Nova, La Rochelle, France).

Statistical Analysis

Comparisons of the survival distributions for scrapie, C-BSE, and H-BSE between transgenic mice overexpressing A53T human α-synuclein (TgM83) and nontransgenic C57BL/6 controls were assessed by applying log-rank tests, and survival curves were obtained by Kaplan-Meier method. Statistical analyses were made with R (*R: A Language and Environment for Statistical Computing*. R Foundation for Statistical Computing, Vienna, Austria. ISBN 3-900051-07-0; URL: http://www.R-project.org).

RESULTS

Reduced Scrapie C506M3, C-BSE, and H-BSE Incubation Periods in TgM83 Mice

The 3 prion strains were inoculated into TgM83 at 6 weeks of age, well before the onset of the motor phenotype associated with mutated α-synuclein overexpression. The incubation periods, that is, the time from the day of inoculation until death (dpi), in TgM83 mice were compared with those of identically inoculated nontransgenic C57BL/6 wt controls (Fig. 1).

For the scrapie C506M3 strain, the incubation period distributions were significantly different ($p < 0.0001$) with a median incubation period of 154 dpi in TgM83 mice versus 177 dpi in C57BL/6 controls (Table). For the C-BSE strain, a significant difference ($p < 0.0001$) was also observed with a median incubation period of 190 dpi in TgM83 mice versus

TABLE. Prion Transmissions (Scrapie C506M3, C-BSE, and H-BSE) to TgM83, C57BL/6, and B6C3H Mice

Prion Strains (% Brain Homogenate Inoculum)		Mouse Strain Host	Mean Incubation Periods (dpi)	No. PrPd-Positive Mice/Total	Positions of the PrPd-Positive Mice in the Cohort and Their Incubation Period (dpi)
Scrapie C506M3	1%	TgM83	154	5/5	1: 139 … 5: 164
	1%	C57BL/6	177	19/19	1: 173 … 19: 184
C-BSE	1%	TgM83	190	8/8	1: 148 … 8: 205
	1%	C57BL/6	204	20/20	1: 194 … 20: 224
	1%	B6C3H	225	10/10	1: 205 … 10: 231
H-BSE	1%	TgM83	444	4/10	7: 515 8: 555 9: 555 10: 609
	1%	C57BL/6	601	3/20	16: 758 18: 791 19: 814
	10%	C57BL/6	555	4/14	6: 503 9: 574 10: 615 13: 667

B6C3H, genetic background of transgenic line TgM83; C57BL/6, wild-type nontransgenic controls; dpi, days post-inoculation.

204 dpi in C57BL/6 mice (Table). C57BL/6 controls developed C-BSE significantly more rapidly than did nontransgenic B6C3H mice ($p < 0.0001$), that is, mice of the same genetic background as TgM83 mice (Table).

The incubation period for TgM83 mice inoculated i.c. with 1% H-BSE was compared with that of C57BL/6 mice infected with the same stock of prion, at either 1% or at 10% (Fig. 1). TgM83 mice inoculated with 1% H-BSE died significantly more rapidly than the identically inoculated C57BL/6 controls ($p = 0.0064$): the median incubation period of 1% H-BSE decreased drastically from 601 dpi in C57BL/6 mice to 441 dpi in TgM83 mice (Table). The distribution of the incubation periods of 1% H-BSE in TgM83 mice was even significantly different from that for C57BL/6 controls inoculated with 10% H-BSE ($p = 0.0351$): the median incubation period of 1% H-BSE in TgM83 was 111 dpi shorter than that of C57BL/6 mice inoculated with 10% H-BSE (Table).

A group of noninoculated TgM83 mice that were killed after the emergence of clinical signs because of the α-synuclein pathology was also included (Fig. 1). There was no difference in survival times between this control group and that of TgM83 mice inoculated with 1% H-BSE ($p = 0.536$). It should be noted that this comparison was of the total survival periods (i.e. period between the birth and death of mice expressed in days after birth), not of the incubation times, because it involved TgM83 mice that were not inoculated (Fig. 1).

All 5 TgM83 mice inoculated with the scrapie strain and 5 of the 8 TgM83 mice inoculated with the C-BSE strain were killed after the onset of clinical signs, whereas the others were found dead. These signs (hunched posture, weight loss, reduced mobility, tail chewing, clasping, and difficulty or inability to stand up) seemed related to prion diseases because, as in the noninoculated aged TgM83 mice, no partial paralysis or stiffness of hind limb and tail was observed. Only 4 of the 10 TgM83 mice inoculated with H-BSE were killed after the development of clinical signs (hunched posture, weight loss, tremor, prostration, and, for 1 mouse, an inability to stand up). In view of this limited number of mice and this mixed symptoms, it was difficult to determine the involvement of prion disease versus α-synuclein pathology in the development of these clinical signs.

Typical Histopathologic and Biochemical Features of Scrapie C506M3, C-BSE, and H-BSE Prion Strains in Inoculated TgM83 Mice

On the basis of immunohistochemical and biochemical analyses, all TgM83 mice inoculated with scrapie C506M3 or C-BSE were positive for PrPd. In contrast, among the 10 TgM83 mice inoculated with 1% H-BSE, only 4 mice (dead at positions 7, 8, 9, and 10; i.e. dpi 515, 555, 555, and 609, respectively) exhibited accumulation of PrPd (Table). In comparison, 3 of the 20 C57BL/6 controls inoculated with 1% H-BSE (dead at positions 16, 18, and 19, i.e. dpi 758, 791, and 814, respectively) were PrPd-positive (Table). Thus, inoculation of TgM83 mice with 1% H-BSE led to an initial accumulation of PrPd that was identified 243 days earlier than in the C57BL/6 control mice inoculated under the same conditions.

Mice inoculated with each of the 3 prion strains showed typical vacuolar lesions. After C-BSE transmission in TgM83 mice, vacuolar lesions were mainly observed in brain areas 1-4-7 (dorsal medulla nuclei, hypothalamus, septal nuclei). Remarkably, the typical vacuolation of the cochlear nucleus usually found in C57BL/6 mice infected with C-BSE was also seen (Fig. 2A). The scrapie C506M3 strain induced milder vacuolar lesions that were more widely distributed in the brains of TgM83 mice (Fig. 2A). In addition to this extensive spongiosis, brains infected with scrapie C506M3 or C-BSE both exhibited typical reactive astrogliosis and PrPd accumulations as fine granular deposits and small plaques (Fig. 2A). In contrast, histologic analyses of PrPd-positive TgM83 mice inoculated with H-BSE revealed no or very minimal vacuolar lesions. Remarkably, PrPd deposits were detected only in the shape of amyloid plaques as shown by Congo red staining observed under polarized light (Fig. 2A). Reactive gliosis was also detected in these infected TgM83 mice (Fig. 2A).

After proteinase K treatment and Western blot analyses of TgM83 brains inoculated with C-BSE, 3 bands corresponding to the nonglycosylated (19.0 kDa), monoglycosylated (22.8 kDa), and biglycosylated (26.0 kDa) forms of the PrP^{res} were detected with antibody Sha31 (Fig. 2B). Similarly, TgM83 mice inoculated with scrapie C506M3 presented the expected profile in which the apparent molecular mass (19.7 kDa) of the nonglycosylated band was higher than in C-BSE (19.0 kDa) (Fig. 2B). The biglycosylated-to-monoglycosylated glycoform ratios of scrapie C506M3 and C-BSE in TgM83 mice (means of 51/37 and 65/27, respectively) remained similar to those obtained in their respective C57BL/6 controls (means of 50/37 and 61/28) (Fig. 2B). As in C57BL/6 mice, these glycoform ratios were lower in scrapie than in C-BSE samples in TgM83 mice. Further Western blot analyses with mAb 12B2 also showed that the molecular features of scrapie C506M3 and C-BSE were conserved after a first passage through TgM83 mice: the usual 3-band profile was obtained for the scrapie strain C506M3, whereas no immunoreactivity was observed in TgM83 mice infected with C-BSE (Fig. 2C).

Biochemical studies of PrP^{res}-positive TgM83 mice inoculated with 1% H-BSE showed molecular features consistent with those previously described for H-BSE, that is, the apparent molecular mass of the 3 PrP^{res} glycoforms was 1.5 kDa higher than that found in mice infected with a C-BSE isolate (Fig. 2D). In addition, a more C-terminally cleaved fragment of PrP^{res} (PrP^{res} #2), with an unglycosylated form migrating at 14 kDa, was also detected by SAF84, an antibody directed against the C-terminal part of the prion protein (Fig. 2D). Finally, the same molecular pattern, characteristic of the H-BSE prion strain, was found in brains of PrP^{res}-positive C57BL/6 mice inoculated either with 1% or with 10% H-BSE (Fig. 2D).

TgM83 Mice Infected With Scrapie C506M3 or C-BSE Do Not Exhibit α-Synuclein Pathology Whereas Concomitant Alterations of Prion Protein and α-Synuclein Are Observed in TgM83 Mice Inoculated With H-BSE

Western blot analysis of symptomatic TgM83 mice killed at 14 months of age showed considerable amounts of

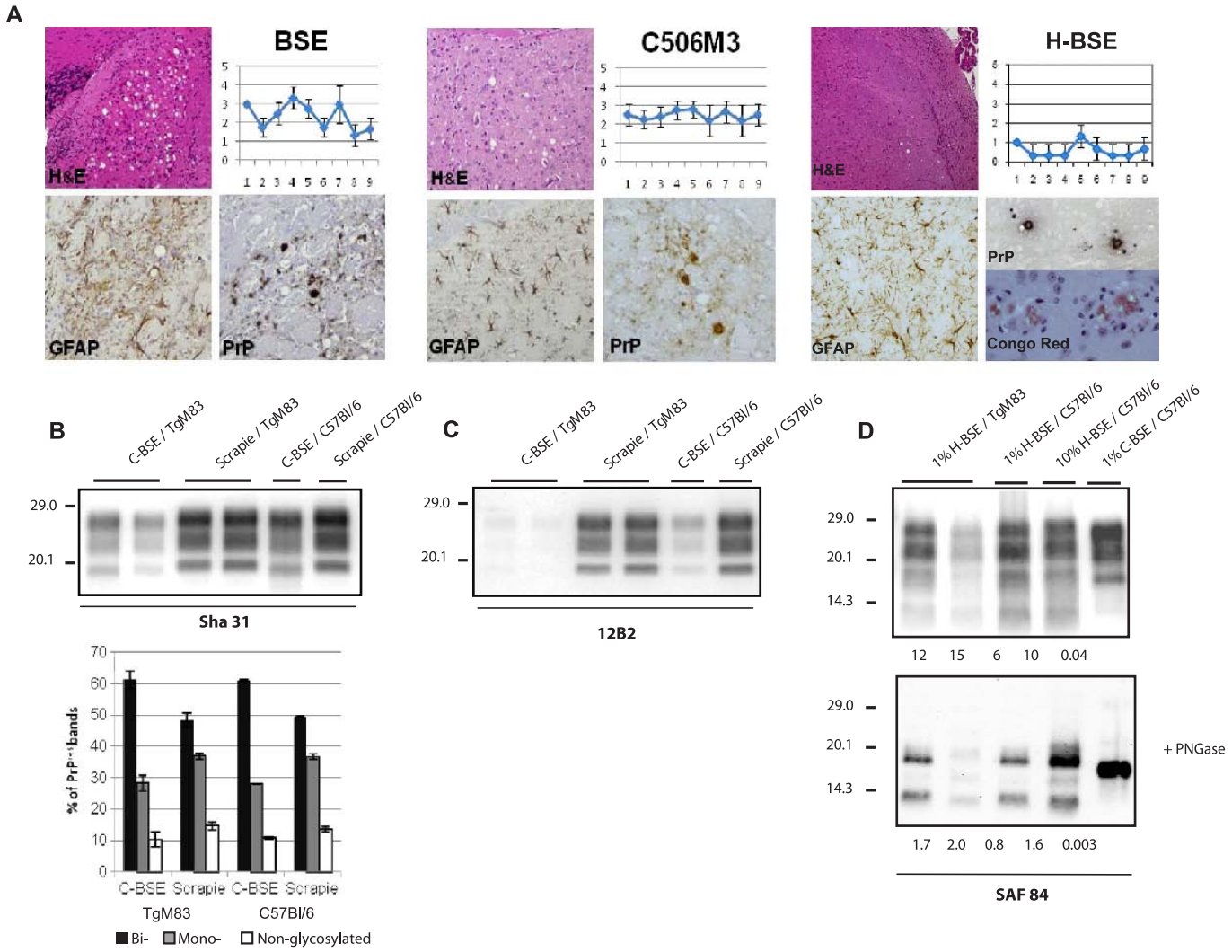

FIGURE 2. Classic-type bovine spongiform encephalopathy (C-BSE), scrapie C506M3, and H-type bovine encephalopathy (H-BSE) prion strains maintain their usual histopathologic and biochemical characteristics after a passage in TgM83 mice. **(A)** Neuropathology of TgM83 mice inoculated at first passage either with C-BSE (left panel), scrapie C506M3 (middle panel), or H-BSE (right panel) strains from C57BL/6 mice. Hematoxylin and eosin (H&E)–stained brain sections reveal typical vacuolar lesions shown in the cochlear nucleus for C-BSE and H-BSE and in the septum for C506M3 strain. The respective lesion profiles were established from the H&E-stained sections. 1, dorsal medulla nuclei; 2, cerebellar cortex; 3, superior colliculus; 4, hypothalamus; 5, central thalamus; 6, hippocampus; 7, septal nuclei; 8, cerebral cortex at the thalamus; 9, cerebral cortex at the septal nuclei. Glial fibrillary acidic protein (GFAP) immunostaining indicated the occurrence of gliosis, shown in the striatum (stellate brown-colored labeling) in each experiment. Immunohistochemical analyses of PrPd with monoclonal antibody SAF84 showed fine granular deposits and small plaques for C-BSE and scrapie C506M3 (illustrated in the striatum), whereas only typical amyloid plaques were found in the thalamus for H-BSE (consistent with the birefringence after Congo red staining observed under polarized light). **(B, C)** Brain PrP^{res} from TgM83 mice and C57BL/6 controls inoculated with C-BSE or with scrapie C506M3 strains detected by Western blot with Sha31 **(B)** or 12B2 **(C)** antibodies. Brain tissue aliquots (20 μg) were loaded by lane except for the second TgM83 mouse inoculated with C-BSE for which 40 μg was loaded. Mean percentages (±SD) of the 3 PrP^{res} bands are shown on the graph (biglycosylated band in black bars, mono-glycosylated band in gray bars, and nonglycosylated band in white bar). **(D)** Brain PrP^{res} from TgM83 and C57BL/6 mice, inoculated either with 1% or with 10% H-BSE brain homogenates detected by SAF84. The quantities of brain homogenates in milligrams loaded per well are indicated under each lane.

phosphorylated α-synuclein in the detergent-insoluble fraction (Fig. 3). The molecular pattern associated with these altered forms of α-synuclein was composed of (i) a main band at 18 kDa corresponding to monomeric α-synuclein, (ii) a second band at 24 kDa that might represent mono-ubiquitinated α-synuclein, and (iii) high-molecular weight forms of α-synuclein (Fig. 3). Conversely, no phosphorylated insoluble form of α-synuclein was detected in brains of non-inoculated TgM83

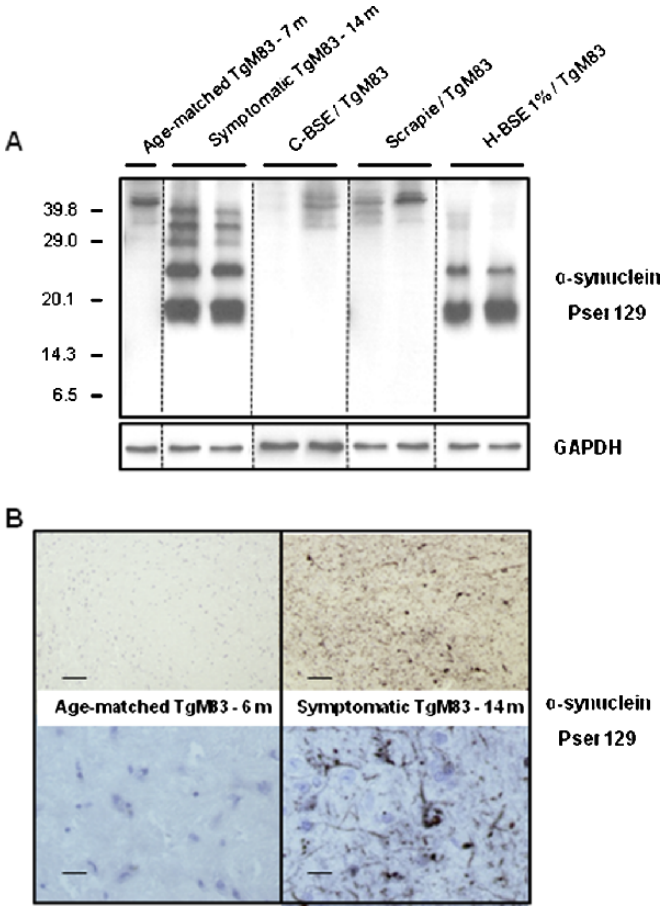

FIGURE 3. TgM83 mice inoculated with H-type bovine spongiform encephalopathy (H-BSE) prion strain develop α-synuclein alterations, whereas no pathological forms of α-synuclein are detected in mice that died of scrapie C506M3 or classical bovine spongiform encephalopathy (C-BSE). **(A)** Insoluble and phosphorylated forms of α-synuclein from TgM83 mice inoculated with C-BSE, scrapie C506M3, or H-BSE were detected by Western-blot with an anti–Pser129 α-synuclein antibody. Symptomatic 14-month-old and asymptomatic 7-month-old TgM83 mice are included as non-inoculated controls. Immunodetection of a ubiquitous protein (GAPDH) confirmed that comparative amounts of proteins were loaded in the lanes. **(B)** Upper panel: low-power light microscopy of phosphorylated α-synuclein detected by immunohistochemistry with anti–Pser129 α-synuclein antibody. Bar = 60 μm. There is no staining in the brain of a control asymptomatic 6-month-old TgM83 mouse. Accumulation of phosphorylated α-synuclein is detected in non-inoculated but symptomatic 14-month-old TgM83 mouse. Higher magnification (lower panel) illustrates typical perikaryal cytoplasmic and neuronal process staining. Bar = 16 μm.

mice killed at 7 months of age or in mice that died because C506M3 or C-BSE prion infection, before development of the clinical signs associated with synucleinopathy (Fig. 3).

TgM83 mice inoculated with prion strains of scrapie C506M3 (dead at ~6.5 months of age) or C-BSE (dead at ~7.5 months of age) did not demonstrate any insoluble form of phosphorylated α-synuclein by Western blot (Fig. 3A). This result suggested that the drastic molecular alterations of human α-synuclein specific to an advanced stage of synucleinopathy had not yet occurred in mice inoculated with scrapie C506M3 or C-BSE at the time of death.

By contrast, the same molecular alterations of α-synuclein were observed in all TgM83 mice inoculated with H-BSE, whether they were PrPd-positive or not. Western blot analyses showed an accumulation of insoluble phosphorylated α-synuclein as in symptomatic TgM83 mice that died at the same time (i.e. at 14 months of age) (Fig. 3A). Similarly, accumulation of phosphorylated α-synuclein was not seen in young control TgM83 mice but was clearly detected in control noninoculated symptomatic TgM83 mice (Fig. 3B) and in H-BSE inoculated TgM83 mice as well (data not shown).

DISCUSSION

Neurodegenerative diseases are often associated with the misfolding and deposition of neuronal proteins, such as β-amyloid peptide and τ protein in Alzheimer disease, prion protein in TSEs, and α-synuclein in PD and related disorders. Because the simultaneous presence of several of these damaged proteins has been commonly observed in association with the same pathological findings (22, 23, 34–39), recent studies have investigated their possible molecular interactions. Indeed, hybrid complexes involving A-β peptide with τ protein (40), α-synuclein (41, 42), or prion protein (43) have been demonstrated. In addition, τ- and α-synuclein can self-associate and promote their own polymerization into fibrils (21, 44–46).

Few data have been published regarding the occurrence of potential interactions between prion protein and α-synuclein in neurodegenerative diseases. Moreover, 2 previous immunohistochemical analyses of various cases of prion diseases (human patients with CJD, sheep and goats with natural scrapie, or hamsters experimentally inoculated with prions) revealed the existence of immunoreactive α-synuclein deposits in the brains but with no obvious colocalization of PrPd and α-synuclein (24, 26). Conversely, detailed neuropathological studies of genetic cases of CJD have recently highlighted intense neurodegeneration associated with deposits of proteins, including α-synuclein, but typical Lewy bodies and Lewy neurites were only identified in 6 (15.4%) of the 39 cases studied with an E200K mutation; 13 other cases showed prominent neuronal granular diffuse cytoplasmic immunoreactivity in some brain areas (22). Recent experiments have demonstrated that the accumulation of PrPd, synaptic loss, and behavioral dysfunction associated with the murine scrapie strain ME7 are not modified by spontaneous deletion of the α-synuclein gene *snca* harbored by a substrain of C57BL/6 mice (47). These findings led the authors to conclude that α-synuclein deficiency does not contribute to the compartment-specific processes that give rise to prion disease–mediated synaptotoxicity and neurodegeneration (47). Consequently, the question as to whether prion protein and α-synuclein alterations affect each other remains of interest and requires further experimental investigations.

To trigger a prion disease concomitantly with a synucleinopathy, transgenic mice overexpressing human A53T α-synuclein were challenged i.c. with 3 different prion strains. Such transgenic mice spontaneously displayed age-dependent

motor impairment when the animals are 10 to 22 months old. The onset of clinical disease was associated with the development of amyloidogenic, filamentous intraneuronal inclusions of α-synuclein that mirror many of the histopathologic and biochemical features of human synucleinopathies (27, 48, 49). Here, our Western blot analysis confirmed that the pathological forms of α-synuclein in the mouse brains had the same molecular characteristic as that observed in the human disease, that is, the altered α-synuclein extracted from symptomatic TgM83 mice was detergent-insoluble and phosphorylated on serine residue 129 (50–52). A reliable correlation between disease development and the detection of insoluble Pser129 α-synuclein, including species with retarded electrophoretic mobility, was reported in mice that overexpress human A30P α-synuclein, another mouse model of synucleinopathy (53). The TgM83 murine model was chosen for this study because the clinical and molecular changes occurring during the aging of these mice provide reliable criteria distinct from those known in prion diseases for the specific detection of α-synuclein–associated alterations. However, it would also be relevant to carry out inoculations with prions in transgenic mice expressing human wt α-synuclein (instead of a mutated form) to develop a model that reproduces the potential pathological relationship that might occur between prion and α-synuclein in sporadic CJD.

We found that scrapie C506M3 and C-BSE incubation periods were greatly decreased in TgM83 mice in comparison to those of identically non-transgenic C57BL/6 controls. In contrast, all the TgM83 mice inoculated with scrapie C506M3 or C-BSE died of prion disease before the onset of detectable insoluble α-synuclein phosphorylated on serine 129. To trigger a prion disease synchronously with an α-synuclein pathology, scrapie C506M3 and C-BSE prion strains could also be inoculated intraperitoneally into TgM83 mice, which would lead to delayed onset of these prion diseases (54).

TgM83 mice were also inoculated with 1% H-BSE, an atypical bovine strain that possesses a longer incubation period than scrapie C506M3 and C-BSE in C57BL/6 mice (55). The median incubation period of TgM83 mice inoculated with 1% H-BSE was significantly shorter than that of C57BL/6 controls infected with the same agent either at 1% or at 10%. Transmission of H-BSE did not change the total life span of TgM83 mice, that is, statistical analyses failed to show any significant difference between the median incubation period of TgM83 mice inoculated with 1% H-BSE and that of noninoculated TgM83 mice. All TgM83 mice inoculated with H-BSE had α-synuclein molecular alterations typical of an advanced stage of synucleinopathy (i.e. insoluble and phosphorylated on serine 129 residue). Moreover, PrPd accumulations were observed in the last 4 mice of the cohort that died of 515 dpi onward (earlier than C57BL/6 controls inoculated with 1% H-BSE). Thus, these 4 TgM83 mice exhibited a prion disease alongside extensive α-synuclein pathology. It should be noted that a similarly low attack rate was found after inoculation of C57BL/6 mice with the same brain homogenate and that this differed strikingly from the high attack rate previously reported after inoculations of C57BL/6 mice with an inoculum produced from another mouse inoculated with the same H-BSE isolate (03-2095) (55). As previously done for scrapie and C-BSE strains in C57BL/6 (54, 56), further measurements of the PrPd amounts in brains of inoculated TgM83 mice over time would be informative in this context.

It seems unlikely that the reduction of the incubation periods of scrapie C506M3, C-BSE, and H-BSE in TgM83 mice was linked to changes in the properties of prion strains. No modification in the histopathologic and molecular features of these 3 prion strains was observed in TgM83 mice compared with the C57BL/6 mice. All TgM83 mice inoculated with scrapie C506M3 and C-BSE had the same molecular characteristics (immunoreactivity, glycoform ratios) and lesion profiles as those described in infected C57BL/6 mice (12, 28, 57). The pathological forms of prion, apparent from 515 dpi in TgM83 mice inoculated with H-BSE, showed similar molecular features and brain lesions to those observed in C57BL/6 mice after a first passage of the same inoculum (29, 58). These molecular features were also identical to those described in cattle (59, 60) or in bovine transgenic mice (61) with H-type BSE. Conversely to what was recently reported in a few mice during some second passages of the same H-BSE isolate, no emergence of C-BSE properties was observed here (55). Nonetheless, possible changes of the infectious agents in TgM83 mice cannot be fully excluded based solely on phenotypic characterization of the resulting disease. To verify this, we would have to transmit the disease from TgM83 mice to C57BL/6 mice, the previous hosts of these TSEs. Indeed, previous studies have suggested that the virulence of prion agents can be modified even if the biochemical signature, lesion profile, and PrPd deposition pattern of a prion strain are similar, at least after crossing a species barrier (62).

The reduced incubation periods observed in prion inoculated TgM83 mice might also not be due to their genetic background: statistical analyses showed that B6C3H mice (i.e. the TgM83 genetic background) developed C-BSE significantly slower than C57BL/6 controls. However, the remote possibility that the insertion of the α-synuclein transgene into the genome of TgM83 mice had modified their genetic susceptibility to prion disorders could not be totally excluded (63).

The early onset of neurologic disease in TgM83 mice inoculated with scrapie C506M3 or C-BSE prion strains occurred independently of the presence of detectable altered forms of α-synuclein specific to an advanced stage of synucleinopathy. It is possible that our Western blot analyses was not sufficiently sensitive to detect very low levels of insoluble and phosphorylated forms of α-synuclein; such forms might be sufficient to increase the neuronal susceptibility to prion infection. Whereas this last form of the protein is only detectable at the late stage of the disease, other yet uncharacterized pathological forms of the protein could also be present at earlier stages. We cannot exclude the possibility that molecular interactions exist between PrPd and such other forms of pathological α-synuclein. Speculatively, it is conceivable that α-synuclein, which can be both soluble in the cytoplasm (64) or bound to membranes via the formation of N-terminal α helices (65), would influence conversion of PrPc into PrPd, an event that occurs in membrane-bound vesicles (66).

Direct interaction between the α-synuclein and prion proteins is, however, not necessarily required to explain our results and we propose several possible mechanisms that could explain earlier disease in TgM83 mice inoculated with scrapie or classic BSE. Overburden of the proteasome system and/or of the lysosomal pathway in a mouse brain faced with an overproduction of misfolded proteins might lead to an aggravation of the pathology (67–70). Impairment of the ubiquitin-proteasome system in neurons has been described in a mouse model overexpressing the A53T α-synuclein (71), and a relationship between α-synuclein oligomers and inhibition of proteasome activities was shown in vitro (72). Such impairment could directly explain shortened survival after prion infection of mice overexpressing the A53T α-synuclein. Other possibilities would be that PrPd and pathological α-synuclein could act concomitantly to induce oxidative stress, membrane disruption, and mitochondrial impairments that might initiate the synaptic pathology common to these 2 diseases (73–77). Using recombinant adenoassociated virus 2–mediated delivery of A53T human α-synuclein, it was shown that levels of proteins involved in synaptic transmission and axonal transport were altered at early stages of disease progression, well before neuronal cell death occurs (78). Interestingly, a recent study using lentivirus-based expression of α-synuclein variants showed the high in vivo toxicity of membrane-associated oligomers from variants prone to oligomerization, whereas variants that formed fibrils were less toxic; the mechanism of toxicity was linked to alterations in the permeability and integrity of the cell membrane (79). Similar mechanisms might facilitate the development of prion diseases in mice with mutated α-synuclein before the advanced stage of synucleinopathy.

In conclusion, we demonstrate that some transgenic mice overexpressing human A53T α-synuclein and inoculated with H-BSE PrPd i.c. developed a prion disease alongside the synucleinopathy. More generally, our study is the first description of a model aimed at defining the potential linkage between PrPd and α-synuclein.

ACKNOWLEDGMENTS

The authors thank Dominique Canal for the Western blot experiments; Céline Raynaud and Mikaël Leboidre for excellent histotechnical assistance; and Emilie Antier, Coralie Pulido, and Damien Gaillard for performing animal experiments.

REFERENCES

1. Glabe CG. Common mechanisms of amyloid oligomer pathogenesis in degenerative disease. Neurobiol Aging 2006;27:570–75
2. Soto C, Estrada LD. Protein misfolding and neurodegeneration. Arch Neurol 2008;65:184–89
3. Saha AR, Ninkina NN, Hanger DP, et al. Induction of neuronal death by α-synuclein. Eur J Neurosci 2000;12:3073–77
4. Cookson MR. α-Synuclein and neuronal cell death. Mol Neurodegener 2009;4:9
5. Kopito RR. Aggresomes, inclusion bodies and protein aggregation. Trends Cell Biol 2000;10:524–30
6. Morimoto RI. Proteotoxic stress and inducible chaperone networks in neurodegenerative disease and aging. Genes Dev 2008;22:1427–38
7. Prusiner SB. Novel proteinaceous infectious particles cause scrapie. Science 1982;216:136–44
8. Baron T, Bencsik A, Vulin J, et al. A C-terminal protease-resistant prion fragment distinguishes ovine "CH1641-like" scrapie from bovine classical and L-Type BSE in ovine transgenic mice. PLoS Pathog 2008;4: e1000137
9. Bencsik A, Baron T. Bovine spongiform encephalopathy agent in a prion protein (PrP)ARR/ARR genotype sheep after peripheral challenge: Complete immunohistochemical analysis of disease-associated PrP and transmission studies to ovine-transgenic mice. J Infect Dis 2007;195: 989–96
10. Bruce ME. Strain Typing Studies in Scrapie and BSE. In: Baker H, Ridley RM, eds. *Methods in Molecular Medicine. Prion Diseases, vol. 3*. Totowa, NJ: Humana Press, 1996:223–36
11. Brown DA, Bruce ME, Fraser JR. Comparison of the neuropathological characteristics of bovine spongiform encephalopathy (BSE) and variant Creutzfeldt-Jakob disease (vCJD) in mice. Neuropathol Appl Neurobiol 2003;29:262–72
12. Baron T, Crozet C, Biacabe AG, et al. Molecular analysis of the protease-resistant prion protein in scrapie and bovine spongiform encephalopathy transmitted to ovine transgenic and wild-type mice. J Virol 2004;78:6243–51
13. El-Agnaf OM, Jakes R, Curran MD, et al. Effects of the mutations Ala30 to Pro and Ala53 to Thr on the physical and morphological properties of α-synuclein protein implicated in Parkinson's disease. FEBS Lett 1998; 440:67–70
14. Polymeropoulos MH, Lavedan C, Leroy E, et al. Mutation in the α-synuclein gene identified in families with Parkinson's disease. Science 1997;276:2045–47
15. Singleton AB, Farrer M, Johnson J, et al. α-Synuclein locus triplication causes Parkinson's disease. Science 2003;302:841
16. Chartier-Harlin MC, Kachergus J, Roumier C, et al. α-Synuclein locus duplication as a cause of familial Parkinson's disease. Lancet 2004;364: 1167–69
17. Greenbaum EA, Graves CL, Mishizen-Eberz AJ, et al. The E46K mutation in α-synuclein increases amyloid fibril formation. J Biol Chem 2005; 280:7800–7
18. Ibanez P, Bonnet AM, Debarges B, et al. Causal relation between α-synuclein gene duplication and familial Parkinson's disease. Lancet 2004;364:1169–71
19. Spillantini MG, Schmidt ML, Lee VM, et al. α-Synuclein in Lewy bodies. Nature 1997;388:839–40
20. Shults CW. Lewy bodies. Proc Natl Acad Sci U S A 2006;103:1661–68
21. Giasson BI, Lee VM, Trojanowski JQ. Interactions of amyloidogenic proteins. Neuromol Med 2003;4:49–58
22. Kovacs GG, Seguin J, Quadrio I, et al. Genetic Creutzfeldt-Jakob disease associated with the E200K mutation: Characterization of a complex proteinopathy. Acta Neuropathol 2010;121:39–57
23. Kovacs GG, Botond G, Budka H. Protein coding of neurodegenerative dementias: The neuropathological basis of biomarker diagnostics. Acta Neuropathol 2010;119:389–408
24. Haik S, Privat N, Adjou KT, et al. α-Synuclein–immunoreactive deposits in human and animal prion diseases. Acta Neuropathol 2002;103: 516–20
25. Vital A, Fernagut PO, Canron MH, et al. The nigrostriatal pathway in Creutzfeldt-Jakob disease. J Neuropathol Exp Neurol 2009;68:809–15
26. Adjou KT, Allix S, Ouidja MO, et al. α-Synuclein accumulates in the brain of scrapie-affected sheep and goats. J Comp Pathol 2007;137:78–81
27. Giasson BI, Duda JE, Quinn SM, et al. Neuronal α-synucleinopathy with severe movement disorder in mice expressing A53T human α-synuclein. Neuron 2002;34:521–33
28. Lezmi S, Bencsik A, Baron T. PET-blot analysis contributes to BSE strain recognition in C57BL/6 mice. J Histochem Cytochem 2006;54: 1087–94
29. Biacabe AG, Jacobs JG, Bencsik A, et al. H-type bovine spongiform encephalopathy: Complex molecular features and similarities with human prion diseases. Prion 2007;1:61–68
30. Fraser H, Dickinson AG. The sequential development of the brain lesion of scrapie in three strains of mice. J Comp Pathol 1968;78:301–11
31. Bencsik A, Philippe S, Vial L, et al. Automatic quantitation of vacuolar lesions in the brain of mice infected with transmissible spongiform encephalopathies. J Virol Methods 2005;124:197–202
32. Lezmi S, Bencsik A, Monks E, et al. First case of feline spongiform encephalopathy in a captive cheetah born in France: PrP(sc) analysis in

various tissues revealed unexpected targeting of kidney and adrenal gland. Histochem Cell Biol 2003;119:415–22
33. Bencsik AA, Coleman AW, Debeer SO, et al. Amplified immunohistochemical detection of PrPsc in animal transmissible spongiform encephalopathies using streptomycin. J Histochem Cytochem 2006;54: 849–53
34. Selikhova M, Williams DR, Kempster PA, et al. A clinico-pathological study of subtypes in Parkinson's disease. Brain 2009;132:2947–57
35. Small SA, Duff K. Linking Aβ and τ in late-onset Alzheimer's disease: A dual pathway hypothesis. Neuron 2008;60:534–42
36. Muramoto T, Kitamoto T, Koga H, et al. The coexistence of Alzheimer's disease and Creutzfeldt-Jakob disease in a patient with dementia of long duration. Acta Neuropathol 1992;84:686–89
37. Ghoshal N, Cali I, Perrin RJ, et al. Codistribution of amyloid beta plaques and spongiform degeneration in familial Creutzfeldt-Jakob disease with the E200K-129 M haplotype. Arch Neurol 2009;66:1240–46
38. Duda JE, Giasson BI, Mabon ME, et al. Concurrence of α-synuclein and tau brain pathology in the Contursi kindred. Acta Neuropathol 2002;104: 7–11
39. Clinton LK, Blurton-Jones M, Myczek K, et al. Synergistic Interactions between Aβ, tau, and α-synuclein: Acceleration of neuropathology and cognitive decline. J Neurosci 2010;30:7281–89
40. Guo JP, Arai T, Miklossy J, et al. Aβ and tau form soluble complexes that may promote self aggregation of both into the insoluble forms observed in Alzheimer's disease. Proc Natl Acad Sci U S A 2006;103:1953–58
41. Tsigelny IF, Crews L, Desplats P, et al. Mechanisms of hybrid oligomer formation in the pathogenesis of combined Alzheimer's and Parkinson's diseases. PLoS One 2008;3:e3135
42. Masliah E, Rockenstein E, Veinbergs I, et al. β-Amyloid peptides enhance α-synuclein accumulation and neuronal deficits in a transgenic mouse model linking Alzheimer's disease and Parkinson's disease. Proc Natl Acad Sci U S A 2001;98:12245–50
43. Morales R, Estrada LD, Diaz-Espinoza R, et al. Molecular cross talk between misfolded proteins in animal models of Alzheimer's and prion diseases. J Neurosci 2010;30:4528–35
44. Marui W, Iseki E, Ueda K, et al. Occurrence of human α-synuclein immunoreactive neurons with neurofibrillary tangle formation in the limbic areas of patients with Alzheimer's disease. J Neurol Sci 2000;174: 81–84
45. Schmidt ML, Martin JA, Lee VM, et al. Convergence of Lewy bodies and neurofibrillary tangles in amygdala neurons of Alzheimer's disease and Lewy body disorders. Acta Neuropathol 1996;91:475–81
46. Nonaka T, Watanabe ST, Iwatsubo T, et al. Seeded aggregation and toxicity of α-synuclein and tau: Cellular models of neurodegenerative diseases. J Biol Chem 2010;5:34885–98
47. Asuni AA, Hilton K, Siskova Z, et al. α-Synuclein deficiency in the C57BL/6JOlaHsd strain does not modify disease progression in the ME7-model of prion disease. Neuroscience 2009;165:662–74
48. Lee MK, Stirling W, Xu Y, et al. Human α-synuclein–harboring familial Parkinson's disease–linked Ala-53 –> Thr mutation causes neurodegenerative disease with α-synuclein aggregation in transgenic mice. Proc Natl Acad Sci U S A 2002;99:8968–73
49. Waxman EA, Giasson BI. Molecular mechanisms of α-synuclein neurodegeneration. Biochim Biophys Acta 2009;1792:616–24
50. Fujiwara H, Hasegawa M, Dohmae N, et al. α-Synuclein is phosphorylated in synucleinopathy lesions. Nat Cell Biol 2002;4:160–64
51. Anderson JP, Walker DE, Goldstein JM, et al. Phosphorylation of Ser-129 is the dominant pathological modification of α-synuclein in familial and sporadic Lewy body disease. J Biol Chem 2006;281: 29739–52
52. Hasegawa M, Fujiwara H, Nonaka T, et al. Phosphorylated α-synuclein is ubiquitinated in α-synucleinopathy lesions. J Biol Chem 2002;277: 49071–76
53. Fournier M, Vitte J, Garrigue J, et al. Parkin deficiency delays motor decline and disease manifestation in a mouse model of synucleinopathy. PLoS One 2009;4:e6629
54. Lasmezas CI, Deslys JP, Demaimay R, et al. Strain specific and common pathogenic events in murine models of scrapie and bovine spongiform encephalopathy. J Gen Virol 1996;77:1601–9
55. Baron T, Vulin J, Biacabe AG, et al. Emergence of classical BSE strain properties during serial passage of H-BSE in wild-type mice. PLoS One 2011;6:e15839
56. Maignien T, Lasmezas CI, Beringue V, et al. Pathogenesis of the oral route of infection of mice with scrapie and bovine spongiform encephalopathy agents. J Gen Virol 1999;80:3035–42
57. Ritchie DL, Boyle A, McConnell I, et al. Transmissions of variant Creutzfeldt-Jakob disease from brain and lymphoreticular tissue show uniform and conserved bovine spongiform encephalopathy-related phenotypic properties on primary and secondary passage in wild-type mice. J Gen Virol 2009;90:3075–82
58. Baron TG, Biacabe AG, Bencsik A, et al. Transmission of new bovine prion to mice. Emerg Infect Dis 2006;12:1125–28
59. Biacabe AG, Laplanche JL, Ryder S, et al. Distinct molecular phenotypes in bovine prion diseases. EMBO Rep 2004;5:110–15
60. Jacobs JG, Langeveld JP, Biacabe AG, et al. Molecular discrimination of atypical bovine spongiform encephalopathy strains from a geographical region spanning a wide area in Europe. J Clin Microbiol 2007;45:1821–29
61. Nicot S, Baron T. Strain-specific barriers against bovine prions in hamsters. J Virol 2011;85:1906–8
62. Espinosa JC, Andreoletti O, Castilla J, et al. Sheep-passaged bovine spongiform encephalopathy agent exhibits altered pathobiological properties in bovine-PrP transgenic mice. J Virol 2007;81:835–43
63. Lloyd SE, Collinge J. Genetic susceptibility to prion diseases in humans and mice. Curr Genomics 2005;6:1–11
64. Weinreb PH, Zhen W, Poon AW, et al. NACP, a protein implicated in Alzheimer's disease and learning, is natively unfolded. Biochemistry 1996;35:13709–15
65. Kim YS, Laurine E, Woods W, et al. A novel mechanism of interaction between α-synuclein and biological membranes. J Mol Biol 2006;360: 386–97
66. Baron GS, Wehrly K, Dorward DW, et al. Conversion of raft associated prion protein to the protease-resistant state requires insertion of PrP-^{res} (PrP(Sc)) into contiguous membranes. EMBO J 2002;21:1031–40
67. Bennett MC, Bishop JF, Leng Y, et al. Degradation of α-synuclein by proteasome. J Biol Chem 1999;274:33855–58
68. Giasson BI, Lee VM. Are ubiquitination pathways central to Parkinson's disease? Cell 2003;114:1–8
69. Zhang NY, Tang Z, Liu CW. α-Synuclein protofibrils inhibit 26S proteasome–mediated protein degradation: Understanding the cytotoxicity of protein protofibrils in neurodegenerative disease pathogenesis. J Biol Chem 2008;283:20288–98
70. Eriksen JL, Dawson TM, Dickson DW, et al. Caught in the act: α-synuclein is the culprit in Parkinson's disease. Neuron 2003;40:453–56
71. Lin X, Parisiadou L, Gu XL, et al. Leucine-rich repeat kinase 2 regulates the progression of neuropathology induced by Parkinson's-disease-related mutant α-synuclein. Neuron 2009;64:807–27
72. Emmanouilidou E, Stefanis L, Vekrellis K. Cell-produced α-synuclein oligomers are targeted to, and impair, the 26S proteasome. Neurobiol Aging 2010;31:953–68
73. Hsu LJ, Sagara Y, Arroyo A, et al. α-Synuclein promotes mitochondrial deficit and oxidative stress. Am J Pathol 2000;157:401–10
74. Siskova Z, Mahad DJ, Pudney C, et al. Morphological and functional abnormalities in mitochondria associated with synaptic degeneration in prion disease. Am J Pathol 2010;177:1411–21
75. Fuhrmann M, Mitteregger G, Kretzschmar H, et al. Dendritic pathology in prion disease starts at the synaptic spine. J Neurosci 2007;27:6224–33
76. Sulzer D. Clues to how α-synuclein damages neurons in Parkinson's disease. Mov Disord 2010;25(Suppl 1):S27–31
77. Smith WW, Jiang H, Pei Z, et al. Endoplasmic reticulum stress and mitochondrial cell death pathways mediate A53T mutant α-synuclein–induced toxicity. Hum Mol Genet 2005;14:3801–11
78. Chung CY, Koprich JB, Siddiqi H, et al. Dynamic changes in presynaptic and axonal transport proteins combined with striatal neuroinflammation precede dopaminergic neuronal loss in a rat model of AAV α-synucleinopathy. J Neurosci 2009;29:3365–73
79. Winner B, Jappelli R, Maji SK, et al. In vivo demonstration that α-synuclein oligomers are toxic. Proc Natl Acad Sci U S A 2011;108: 4194–9

